Cell Mol Neurobiol
DOI 10.1007/s10571-011-9771-5

ORIGINAL RESEARCH

SorLA in Glia: Shared Subcellular Distribution Patterns with Caveolin-1

Iris K. Salgado · Melissa Serrano · José O. García · Namyr A. Martínez · Héctor M. Maldonado · Carlos A. Báez-Pagán · José A. Lasalde-Dominicci · Walter I. Silva

Received: 22 June 2011 / Accepted: 8 November 2011

Abstract SorLA is an established sorting and trafficking protein in neurons with demonstrated relevance to Alzheimer's disease (AD). It shares these roles with the caveolins, markers of membrane rafts microdomains. To further our knowledge on sorLA's expression and traffic, we studied sorLA expression in various cultured glia and its relation to caveolin-1 (cav-1), a caveolar microdomain marker. RT-PCR and immunoblots demonstrated sorLA expression in rat C6 glioma, primary cultures of rat astrocytes (PCRA), and human astrocytoma 1321N1 cells. PCRA were determined to express the highest levels of sorLA's message. Induction of differentiation of C6 cells into an astrocyte-like phenotype led to a significant decrease in sorLA's mRNA and protein expression. A set of complementary experimental approaches establish that sorLA and cav-1 directly or indirectly interact in glia: (1) co-fractionation in light-density membrane raft fractions of rat C6 glioma, PCRA, and human 1321N1 astrocytoma cells; (2) a subcellular co-localization distribution pattern in vesicular perinuclear compartments seen via confocal imaging in C6 and PCRA; (3) additional confocal analysis in C6 cells suggesting that the perinuclear compartments correspond to their co-localization in early endosomes and the trans-Golgi; and; (4) co-immunoprecipitation data strongly supporting their direct or indirect physical interaction. These findings further establish that sorLA is expressed in glia and that it shares its subcellular distribution pattern with cav-1. A direct or indirect cav-1/sorLA interaction could modify the trafficking and sorting functions of sorLA in glia and its proposed neuroprotective role in AD.

I. K. Salgado · M. Serrano · J. O. García · N. A. Martínez · W. I. Silva (✉)
Department of Physiology, UPR-School of Medicine, University of Puerto Rico, PO Box 365067, San Juan, PR 00936-5067, USA
e-mail: walter.silva@upr.edu

H. M. Maldonado
Department of Pharmacology, Universidad Central del Caribe, School of Medicine, Bayamón, PR, USA

C. A. Báez-Pagán · J. A. Lasalde-Dominicci
Department of Biology, University of Puerto Rico, Río Piedras Campus, Río Piedras, PR, USA

Keywords Alzheimer's disease · Caveolae · Glia · Early endosome · Trans-Golgi network

Introduction

Glia exerts physiological (Hansson and Rönnbäck 2003) and pathophysiological functions during brain injury, tumorigenesis, aging, and neurodegeneration (Eddleston and Mucke 1993; Ridet et al. 1997). During these events, glia may exert opposite "cytoprotective versus cytotoxic" actions, depending on the type of insult, its character, extent, and time point (Eddleston and Mucke 1993; Ridet et al. 1997; Mattson and Chan 2003; Fellin and Carmignoto 2004; Chorna et al. 2004; Sofroniew and Vinters 2010). In Alzheimer's disease (AD), neurodegeneration astrocytes (Mattson and Chan 2003; Selkoe 2004; Mrak and Griffin 2005) surround senile plaques, infiltrate plaque cores (Kato et al. 1998), produce the pro-neurotoxin amyloid precursor protein (APP) (Nagele et al. 2004), and synthesize–secrete the established risk factor apolipoprotein E (ApoE) (Poirier 1994).

A novel receptor for APP and ApoE, the sortilin-related receptor sorLA (LR11 or sorL1), implicated in smooth muscle cell proliferation and invasion (Kanaki et al. 1999), has emerged as an important factor in AD pathogenesis

Published online: 30 November 2011

(Yamazaki et al. 1996; Jacobsen et al. 2002; Motoi et al. 1999; Herz et al. 2009). To date, few studies on sorLA have focused on glia (Motoi et al. 1999; Scherzer et al. 2004; Macdonald et al. 2007). SorLA is a multifunctional, multidomain 250 kDa membrane protein related to LDL receptors' family (Yamazaki et al. 1996; Jacobsen et al. 2002; Herz et al. 2009). A downregulation of sorLA in lymphoblast and brains of AD patients (Scherzer et al. 2004; Offe et al. 2006) has been associated as a sporadic AD risk factor (Andersen et al. 2005) and a late onset Alzheimer disease (LOAD) marker (Rogaeva et al. 2007; Bettens et al. 2008). Also sorLA has been identified as a predictor in progression to AD in mild cognitive impairment (MCI) patients (Sager et al. 2007). Single nucleotide polymorphisms and haplotypes in sorLA are also found in diverse ethnicity AD patients (Lee et al. 2007; Rogaeva et al. 2007, 2009; Kölsch et al. 2009).

Understanding sorLA's role in AD (Huse and Doms 2001; Reid et al. 2007) demands expansion of its studies in glia, and in the importantly emerging membrane raft microdomains (Silva et al. 2007). SorLA functions as a sorting and trafficking protein, preventing formation of amyloidogenic peptides from APP (Offe et al. 2006; Schmidt et al. 2007). Although sorLA moves to the plasmalemma and internalizes via clathrin-dependent endocytosis (Andersen et al. 2005; Nielsen et al. 2007), membrane raft microdomains and raft-associated molecules like the caveolins (Pike 2006; Silva et al. 2007) may participate in this trafficking. Membrane rafts are small (10–200 nm), heterogeneous, highly dynamic, cholesterol- and sphingolipid-enriched domains that compartmentalize cellular processes related to trafficking, signaling, protein sorting, and targeting (Pike 2006). Indeed, membrane raft proteins as caveolins and flotillins have been associated with APP and with different APP processing stages (Ikezu et al. 1998; Nishiyama et al. 1999; Kang et al. 2006; Rajendran and Simons 2009; Reid et al. 2007; Schneider et al. 2008; Silva et al. 2007).

Cav-1 physically associates with APP in three non-neuronal cell lines, while α-secretase-mediated proteolysis of APP was shown to occur in CAV (caveolae microdomains (Ikezu et al. 1998). In addition, the cav-1 protein is up-regulated in the hippocampus (and its mRNA in the frontal cortex) of AD patients, and in hippocampal tissue from ApoE-knockout and aged wild-type mice, and the frontal cortex of AD patients (Gaudreault et al. 2004a). Up-regulation of cav-1 is also seen in senescent human brain, and senescent rat brain membrane raft fractions (Kang et al. 2006). The above cited concomitant changes in both cav-1 and sorLA expressions during AD may be intimately linked to glia. To date, no studies have evaluated in parallel the expression of sorLA in glia, its membrane rafts platform, and glial raft-associated molecules like cav-1. Therefore, it is hypothesized that sorLA in glia shares its subcellular distribution profile with cav-1. The present study demonstrates that sorLA in glia co-compartmentalizes with cav-1, predominantly in intracellular sites suggesting a direct or indirect interaction that may constitute a novel target for the modulation of AD progression.

Materials and Methods

Cell Cultures

C6 glioma cells (Cell Systems, Seattle, WA) grown in Nutrient Mixture Ham's F-10 media containing 10% FBS and 1% antibiotic/antimycotic were routinely propagated as confluent monolayers (Silva et al. 2005). 1321N1 (human astrocytoma), primary cultures of rat astrocytes (PCRA), and primary cultures of rat neurons (PCRN) (obtained from the NIH-NCRR-RCMI-supported Neuronal Glia Culture Facility of Universidad Central del Caribe School of Medicine, Bayamón, PR) were grown in Dulbecco's Modified Eagle media containing 10% fetal bovine serum (FBS) and 1% antibiotic/antimycotic. The cells were routinely propagated as confluent monolayers. Induction of C6 glial cells differentiation into astrocyte-like cells was achieved by the addition of 1 mM dibutyryl cyclic AMP (db-cAMP) and reduction of growth media to 1% FBS (Silva et al. 2005). Cells were seeded on cover slips of dual-chamber slides at $\sim 1 \times 10^4$ cells/well for immunofluorescences or in plates at $\sim 1 \times 10^6$ cells/well for mRNA and protein extraction. The cells were incubated at 37°C, in 5% CO_2.

Real Time RT-PCR

Determination of sorLA expression was done via real time RT-PCR. Primers were designed using Bio-Rad's Beacon Designer 5 software (Bio-Rad Laboratories, Hercules, CA) and the following mRNA sequences: rat sorLA (accession number XM217115), human sorLA (accession number NM003105), and rat GAPDH (accession number AF106860). The following PCR primers were used for the detection of sorLA and GAPDH transcripts: rat sorLA sense primer 5′-*TGTGTAAGAACCGTCAGCAGTGTC*-3′ and antisense primer 5′-*AGTAGTCTCCGCAGTCATCCATCC*-3′ (216 bp); human sorLA sense primer 5′-*TCAGTGGAGACAACA GTAAGG*-3′ and antisense primer 5′ *AGGAGGTGGACA GACAGG*-3′ (318 bp); and, rat GAPDH sense primer 5′-*AACTTTGGCATCGTGGAA*-3′ and antisense 5′-*TACA TTGGGGGTAGGAACAC*-3′ (222 bp). Real time RT-PCR was performed in an iCycler using the iQ SYBR Green Supermix (Bio-Rad Laboratories, Hercules, CA). After optimization of PCR conditions, reactions were conducted with

SYBR Green PCR master mix, 10 μM forward/reverse primers and 100 ng of cDNA. PCR parameters were 95°C for 3 min (required for iTaq DNA polymerase activation), 40 cycles of 95°C for 10 s, and 1 min annealing at 55°C for rat and human sorLA primers. The generation of specific PCR products was confirmed by melt curves and separation of the products over agarose gels. PCR cycle number that generated the first fluorescence signal above threshold (threshold cycle, C_T) was determined, and subsequently, a comparative C_T method (Livak and Schmittgen 2001) using GAPDH for normalization was used to measure relative gene expression as previously described (Silva et al. 2005). Mean values of data from three independent experiments were calculated and plotted as a percentage compared with undifferentiated C6 controls (which were set to 100%). RT-PCR analysis was conducted using the NIH-NIGMS-MBRS-SCORE-supported Molecular Core Facility of the UPR-MSC.

Protein Extraction

Confluent C6 glioma cells culture dishes were placed on ice and washed twice with ice-cold PBS. After PBS was removed, 1 ml was added of ice-cold cell lysis buffer (LB) [NaCl 150 mM, Tris HCl 50 mM pH 8.0, octyl-glucoside 60 mM, EDTA 5 mM, PMSF 0.2 mM, and a protease inhibitors cocktail (100 μg/ml each of leupeptin, antipain, bestatin, chymostatin, and pepstatin A)]. Adherent cells were scrapped off from the culture dish using a cold plastic scrapper. Cells were then centrifuged in a cold microcentrifuge for 20 min at 12,000 rpm. The resulting supernatant was transferred into a new microtube and placed on ice for total protein determination, following the Bio-Rad Protein assay protocol (Bio-Rad Laboratories, Hercules, CA).

Preparation of Caveolin-1-Enriched Membrane Rafts Fractions

Density gradient fractionation procedures under detergent-free conditions were performed as previously described (Silva et al. 1999). Lysis buffer containing 500 mM sodium bicarbonate and a cocktail of protease inhibitors (that included PMSF, antipain, bestatin, leupeptin, chemostatin, pepstatin, and EDTA) was added, the cells were scraped, and then homogenized. Discontinuous gradients were prepared by adjusting the homogenate to 45% sucrose by the addition of 90% sucrose in MBS, overlaying with 4 ml of 35% sucrose in MBS, and 4 ml 5% sucrose in MBS. Samples were centrifuged at $100{,}000\times g$ for 22 h in a SW 40Ti rotor (Beckman Instruments). Gradient fractions (12) were collected (1 ml), washed with MBS, centrifuged at $100{,}000\times g$ for 30 min, the resulting pellets resuspended in urea sample buffer (USB) (4% SDS, 8 M urea, 62 mM EDTA, 5% mercaptoethanol, and 0.015% bromophenol blue), boiled, and equal sample volumes were loaded into SDS-PAGE gels.

Immunoprecipitation

Confluent C6 glioma cells culture dishes were placed on ice and washed twice with ice-cold PBS. After PBS was removed, 1 ml was added of ice-cold LB and a protease inhibitors cocktail (100 μg/ml each of leupeptin, antipain, bestatin, chymostatin, and pepstatin A). Adherent cells were scrapped and the cell suspension transferred to a pre-cooled microcentrifuge tube and incubated in rocking motion at 4°C for 30 min. The suspension was then centrifuged at 4°C for 20 min at 12,000 rpm. The resulting supernatant was transferred into a new microtube and placed on ice for total protein determination. Next, we combined 0.5 mg of the cell suspension and 1 μg of antibody (anti-sorLA or anti-cav-1), and the total volume was made up to a final volume of 1 ml using ice-cold LB. Samples were incubated overnight at 4°C, and then 40 μl of protein A/G beads (Thermo Scientific, Rockford, IL) was added and incubated at 4°C for 2 h. Samples were precipitated at 4°C for 15 s at 12,000 rpm, and the resultant supernatant discarded. The immunocomplex was washed three times with ice-cold immunoprecipitation buffer [NaCl 150 mM, Tris HCl 50 mM pH 8.0, octyl-glucoside 60 mM, and EDTA 5 mM), and then twice with ice-cold TBS (NaCl 150 mM, Tris HCl 50 mM pH 8.0). The resultant immunocomplex was suspended in Laemmli sample buffer (Bio-Rad Labs, Hercules, CA). The samples were separated in a SDS-PAGE and immunoblotted as described below.

Western Blots

For SDS-PAGE and immunoblotting, equal sample volumes from cell protein extracts, gradient fractions, and immunoprecipitates were separated in 6% or 10% SDS polyacrylamide gels, and transferred to PVDF membranes with a Bio-Rad Semi-Dry (Bio-Rad Laboratories, Hercules, CA) (Silva et al. 2005). Membranes were blocked with 3–5% non-fat milk, incubated overnight with primary polyclonal antibody against cav-1 (1:5,000) (Sigma-Aldrich, St. Louis, MO), a monoclonal antibody against flotillin-2 (flot-2) (1:250), a monoclonal antibody for sorLA/LR11 (1:250) (BD Biosciences, San Jose, CA). Subsequently, secondary antibodies: anti-rabbit polyclonal (1:10,000) or anti-mouse monoclonal (1:10,000) (Sigma-Aldrich, St. Louis, MO) were added for 1 h at room temperature (RT). Blots were developed using the enhanced chemiluminescence kit SuperSignal® (Pierce, Rockford, IL), and images obtained using a Bio-Rad Gel Doc 1000 system (Bio-Rad Laboratories, Hercules, CA) (NIH-NIGMS-MBRS-SCORE Molecular Core Facility, UPR-MSC).

Immunocytochemistry

For immunofluorescence studies, culture media were decanted, cells rinsed with PBS, fixed with 100% methanol (−20°C), rinsed with PBS and treated with 100 mM NH_4Cl in PBS to quench free aldehyde groups. Cells were rinsed, permeabilized with 0.1% Triton X-100, and incubated in 2% BSA in PBS to reduce non-specific antibody binding for 30 min. Incubation with primary antibodies against sorLA, early endosome antigen-1 (EEA-1) (BD Biosciences, San Jose, CA), trans Golgi network (TGN-38), and cav-1 (Sigma-Aldrich, St. Louis, MO), and with Alexa-coupled secondary antibodies (Invitrogen, Grand Island, NJ) was done for 1 h each at RT. Slides were washed and mounted with anti-fading medium Slowfade® Antifade Kit (Molecular Probes, Eugene, OR). Laser scanning confocal microscopy (LSCM) studies were done with excitation using a 488-nm Argon/2 laser and/or 633 He/Ne laser, and emission acquired using a BP 500-550 or a LP 650 filter on a Zeiss LSM510 Confocal Microscope. Images were obtained, and analysis was done at the NIH-NCRR-RCMI- and NSF-EPSCOR-supported Confocal Imaging Facility at the University of Puerto Rico, Río Piedras Campus, Río Piedras, PR.

Co-localization Analysis

The three-dimensional co-localization analysis was carried out using the Imaris X.64 6.2.0 software (Bitplane AG, Zurich Switzerland). This software implements an algorithm developed by Costes et al. (2004) based on a spatial statistical approach, which automatically and reproducibly quantifies co-localization, thus eliminating visual bias upon the analysis. Imaris x.64 6.2.0 tests for true co-localization by applying a randomization step before co-localization quantification. The test consists in determining if the probability (*P*-value) that the Pearson's correlation coefficient (*r*) (Manders et al. 1992) calculated for the two channels is significantly greater than that calculated if only random overlap was present. A *P*-value greater than 95% has been chosen as indicative of true co-localization. The thresholds were automatically calculated by iteratively calculating *r* while decreasing thresholds until r are equaled to zero (Costes et al. 2004). Collected z-stacks were background-subtracted by determining the mean intensity of fluorescence outside cells and subtracting this intensity value to the collection of voxels in the image. Costes algorithm (Costes et al. 2004) requires that a region of interest be selected before the automatic calculation of thresholds to delimited the boundary of the cells were selected. Upon automatic calculation of thresholds, "co-localization channels" were generated which highlight co-localized voxels in white and can be combined with the two channels under study to create a merged image.

Statistical Analysis

Mean values of data from at least three independent experiments were subsequently calculated and plotted as a percentage compared with untreated controls (which were set to 100%). Standard errors were calculated by one-way analysis of variance (ANOVA) and by Students' paired *t* test. The significance between groups was further analyzed using the post-hoc Tukey test using Graph Pad Prism software (Graph Pad Software Inc., San Diego, CA).

Results

Determination of SorLA Expression in a Series of Glial Cell Model Systems

Studies on sorLA have primarily focused on neuronal cells. In the present study, evaluation of sorLA mRNA expression was done in a series of glial cell model systems (rat C6 glioma, PCRA and human 1321N1 astrocytoma cells), and in parallel in the human SH-SY5Y neuroblastoma cell line and PCRN. Our results demonstrate that the different human/rat and malignant/non-malignant glial cell model systems, as well as the control human neuroblastoma cell line SH-SY5Y and PCRN, express sorLA's message (Fig. 1a). Amplification curves obtained using specific primers for human and rat sorLA revealed the expression of a primary single reaction product in all glial cells tested (Fig. 1b). In addition, separation of the reaction products using agarose gel electrophoresis revealed products of the corresponding expected sizes for human sorLA (318 bp) and rat sorLA (216 bp) (Fig. 1b). Comparison of the relative levels of transcript expression in the rat cell cultures (Fig. 1c) revealed that PCRA express the highest levels of mRNA when compared to the two C6 cells and PCRN ($N = 3$, $***P \leq 0.001$). No significant difference in transcript expression was found between the human SHSY-5Y neuroblastoma and the human 1321N1 astrocytoma cells.

SorLA's Downregulation During Differentiation of C6 Glioma Cells

Differentiation of the rat C6 glioma cell line using low serum and 1 mM db-cAMP into an astrocyte-like phenotype, as revealed by an increased GFAP expression (Silva et al. 2005) resulted in a significant ($N = 3$, $***P \leq 0.001$) downregulation (~75%) in sorLA's transcript expression after 8-, 24-, and 48-h post-induction of differentiation (Fig. 2). Densitometry analysis of the ~250 kDa sorLA band (Fig. 3b) obtained via immunoblots also demonstrated a significant downregulation of the sorLA's protein in the differentiated phenotype (T_{48}) when compared to

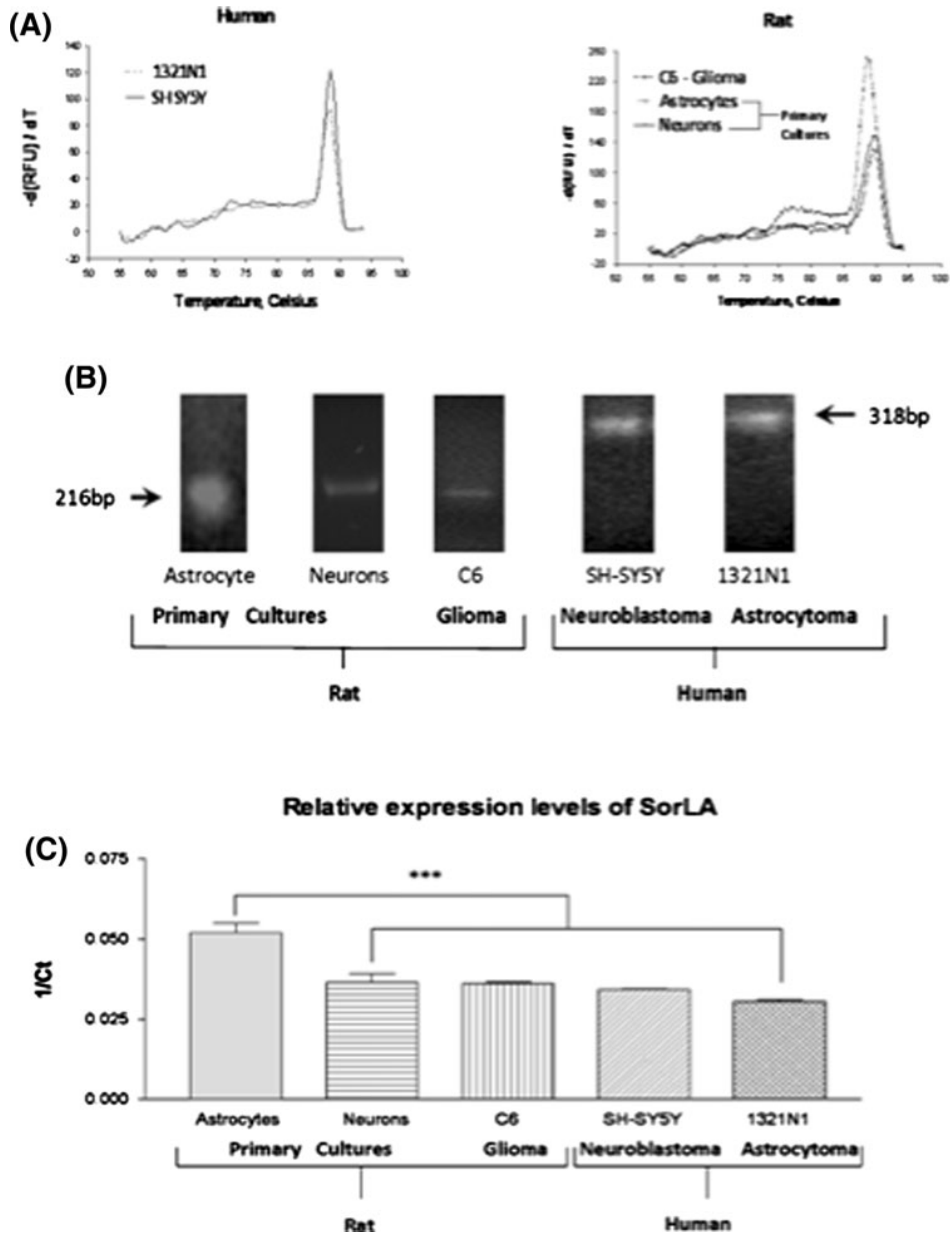

Fig. 1 SorLA's mRNA expression in glia and neuron cells. **a** the real time RT-PCR melt curves for human and rat cells model systems. **b** representative gels confirming the expected size of the amplified sorLA sequence in rat and human cells. **c** the relative expression levels of sorLA in rat cells and human cells, demonstrating a major expression of sorLA in PCRA and similar levels of sorLA in the primary cultures of rat neurons (PCRN) cells, C6 glial cells and human cells (SHSY-5Y and 1321N1 astrocytoma cells). Each *bar* represents the mean ± SEM of at least three experiments ($N = 3$, $^{***}P \leq 0.001$)

undifferentiated (T_0) cells (decrease of 46.1% ± 11.69%; $P \leq 0.01$) (Fig. 3c). The India ink staining (Fig. 3a) was used for total protein content estimates and correction.

SorLA Co-Fractionates with Membrane Rafts Proteins (Cav-1 and Flot-2) Using Density Gradient Centrifugation Under Detergent-Free Conditions

Sucrose density gradient centrifugation under detergent-free conditions was performed to further provide evidence on the expression of sorLA in glial cells, and establish if it co-fractionates with the membrane raft protein cav-1 (Fig. 4). The results corroborate sorLA protein expression in the two C6 phenotypes, and establish its expression in PCRA and 1321N1 astrocytoma cells (fractions 4–5 in Fig. 4a–d). In addition, Fig. 4a–d shows that sorLA also co-fractionates with the membrane raft marker protein flot-2 in light-density membrane raft fractions (fractions 4–5) obtained under detergent-free conditions, in all of the cultured glia tested.

Immunocytochemical Analysis of SorLA Expression in Glia and its Co-Localization with Cav-1

To further the characterization of sorLA in glia, we performed immunofluorescence confocal co-localization analysis in undifferentiated (T_0) cells C6 (Fig. 5, top panel), differentiated C6 (T_{48}) (Fig. 5, middle panel), and

PCRA (Fig. 5, bottom panel). As can be seen, sorLA (green staining) displays a subcellular distribution pattern similar to the one detected in neurons and other cell types (Andersen et al. 2005; Nielsen et al. 2007; Bujo and Saito 2000). In all cases, the immunostaining pattern of sorLA is characterized by a diffuse dotted-punctuate labeling of cytoplasmic vesicles and plasmalemma, with a prominent labeling of larger intracellular vesicular structures. The intracellular and perinuclear labeling exhibited by sorLA has been shown to correspond to its transit via the clathrin-mediated endocytic path to EE and its shuttling to-and-from the trans-Golgi (Offe et al. 2006), assisted by its vps10p domain (Marcusson et al. 1994; Yamazaki et al. 1996; Jacobsen et al. 2002). The cav-1 immunostaining (red) exhibits a subcellular distribution pattern characterized by intensely fluorescent punctae throughout the cytoplasm and diffuse micropatches at the level of the plasmalemma. In all cells analyzed (Fig. 5) a very discrete co-localization was also seen at the level of the plasmalemma (see inserts boxes for each cell type), a region demarked in the sections shown by the presence of the CAV micropatches in C6 (Silva et al. 1999, 2005). Plasmalemma level co-localization pixels were more evident in differentiated C6 cells (Fig. 5, middle panel).

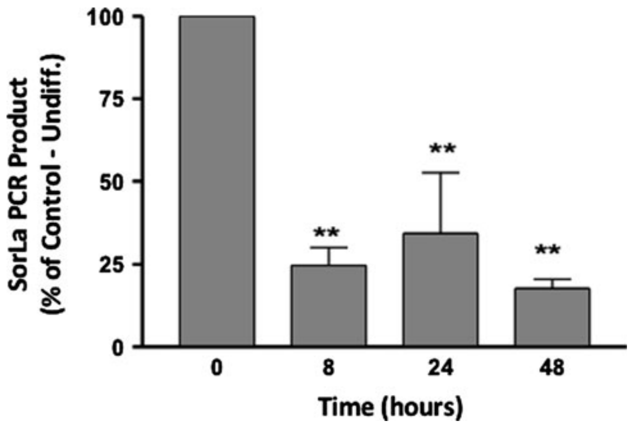

Fig. 2 SorLA's mRNA downregulation in C6 glial cells differentiation and demonstrates that differentiation of C6 cells into an astrocyte-like phenotype results in a significant downregulation of sorLA's mRNA expression after 8, 24 and 48 h post-differentiation induction. Each bar represents the mean ± SEM ($N = 4$, $^{**}P \leq 0.01$)

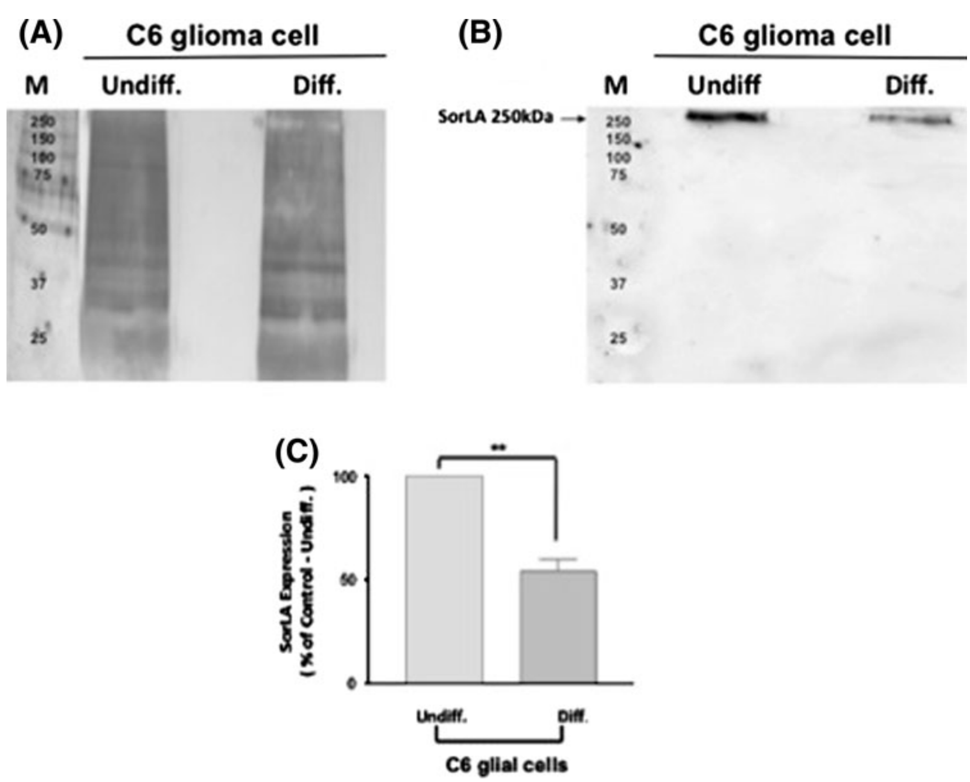

Fig. 3 Western blot analysis of sorLA's expression in undifferentiated (To, control) and differentiated (T48, 48-h post db-cAMP-induced differentiation) C6 glioma cells. **a** represents the India Ink staining of the membrane used to determine the relative protein content. **b** the membranes for the analysis of the 250-kDa band corresponding to the sorLA's expression using 50 μg of protein from total homogenate of C6 glioma cells at undifferentiated and differentiated states induced with db-cAMP along with molecular weight makers (M). Equal amounts of samples were loaded and separated by SDS-PAGE. **c** demonstrates the densitometry analysis for sorLA. Optical density for the specific bands was performed and corrected by protein content. Results represent a 46.1% of change in differentiated phenotype relative to the undifferentiated cells. Each *bar* represents the mean ± SEM of at least four experiments ($N = 4$, $^{**}P \leq 0.01$)

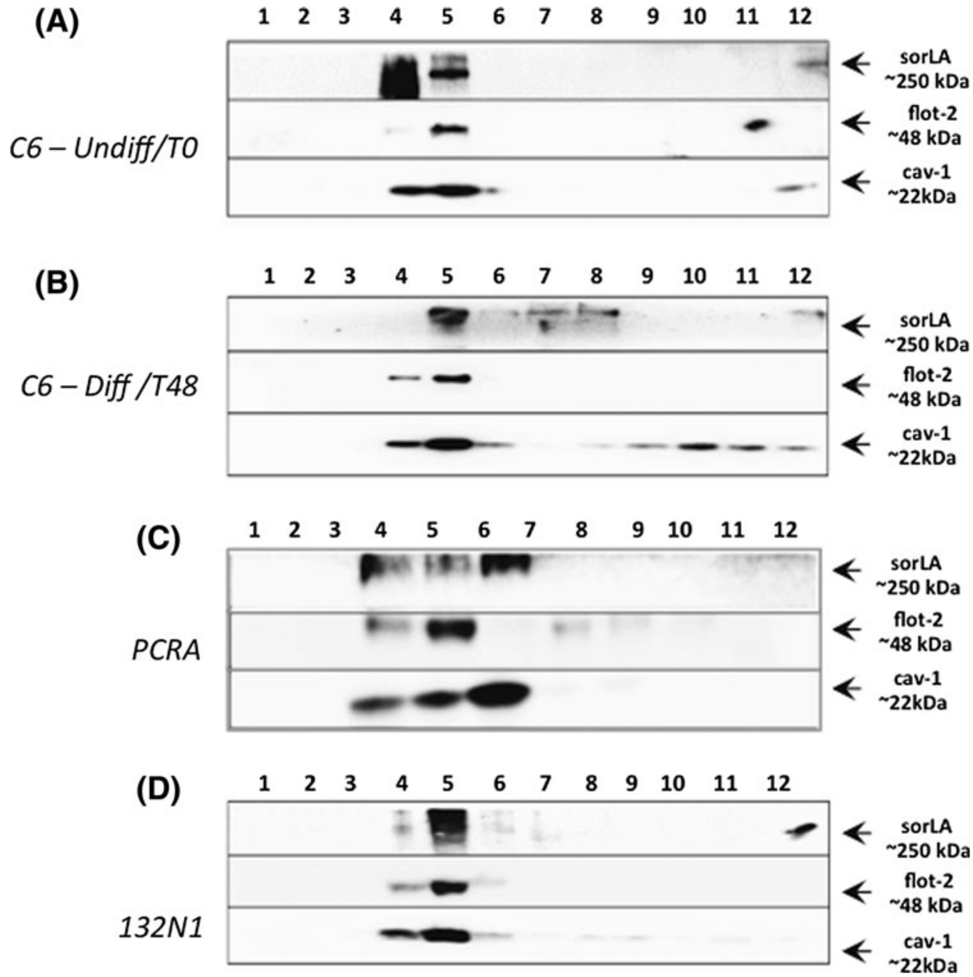

Fig. 4 Membrane rafts subfractionation via sucrose density gradients and detergent-free conditions. Immunoblotting representing the co-fractionation of sorLA with a expected band of $\sim$250 kDa, and the membrane raft markers flotillin-2 and cav-1 with a molecular weight of $\sim$48 and $\sim$22 kDa, respectively are shown for undifferentiated (**a**) and differentiated (**b**) C6 glioma, the human astrocytoma cell line 13121N1 (**c**) and PCRA (**d**). Twelve 1-ml fractions were collected from the *top* (*left side*) to the *bottom* (*right side*). The light-density, membrane raft fractions (fractions 4–5) and caveolin-enriched are defined by intense cav1 and flotillin-2 labeling

Subsequently, to determine the intracellular compartment(s) involved in the observed sorLA and cav-1 co-localization, a LSCM analysis was done in undifferentiated C6 using EEA-1 as a marker for the early endosomal (EE) compartment or TGN-38 for the trans-Golgi (TGN) network. Figure 6a (top) reveals intracellular co-localization between sorLA (green) and EEA-1 (red) in the larger intracellular vesicular structures corresponding to the EE compartment, a result consistent with those reported for sorLA in neurons (Andersen et al. 2005). Similarly, co-localization was also observed between cav-1 (green) and EEA-1 (red) in the larger intracellular vesicular structures corresponding to the EE compartment (Fig. 6a, bottom), as has previously been shown in other cell types. The EE compartment is an intracellular site where both molecules converge. Convergence of sorLA and cav-1 in the TGN is also inferred form the parallel co-localization analysis done using TGN-38 as a marker (Fig. 6b). In this case, the classical perinuclear staining for TGN (Fig. 6b) was observed, and co-localization observed for both sorLA (green) and TGN-38 (red) (Fig. 6b, top), as well as between cav-1 (green) and TGN-38 (red) (Fig. 6b, bottom). Co-localization dots (white panel) and merged (green/red) images in Fig. 6 clearly demonstrate these shared co-localization patterns.

SorLA and Cav-1 Directly or Indirectly Interact as Determined by Immunoprecipitation Analysis

Immunoprecipitation analysis was performed to further provide evidence of a physical (direct or indirect) interaction between sorLA and cav-1 in undifferentiated C6 glioma cells. Figure 7 (left panel) reveals that cav-1 immunoreactivity is detected in immunoprecipitation complexes obtained by the use of beads coupled to either anti-sorLA or anti-cav-1 (positive control) antibodies. While sorLA immunoreactivity (right panel) is also detected in immunoprecipitation complexes obtained using either anti-sorLA (positive control) or anti-cav-1 coupled beads. As a negative control Western blots against cav-1 were done on membranes from immunoprecipitates obtained with beads only (left panel). This immunoprecipitation analysis is consistent with sorLA's co-fractionation in cav-1-positive light-density membrane raft

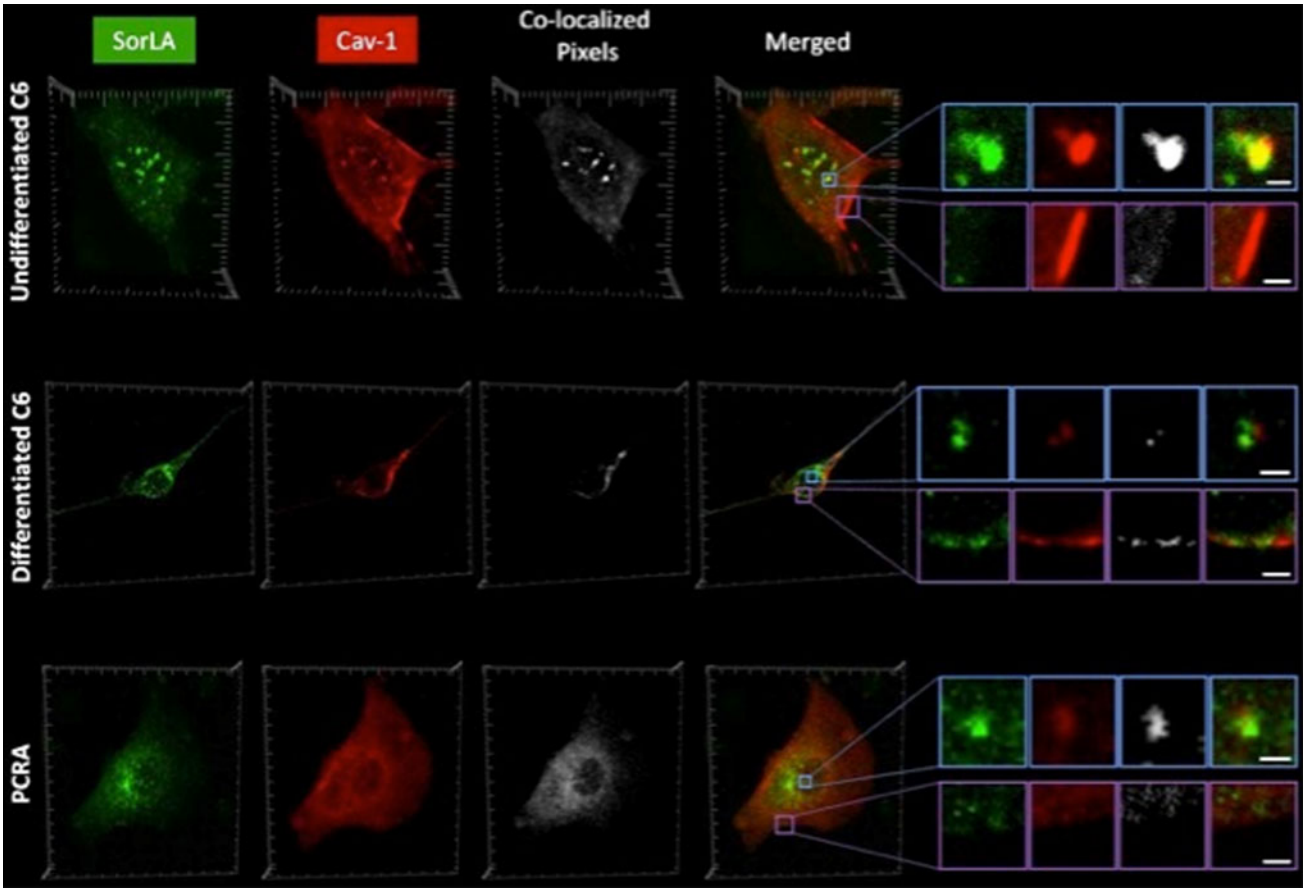

Fig. 5 Immunofluorescence analysis of sorLA and cav-1 in undifferentiated C6 glioma cells (*top panel*), differentiated C6 cells (*middle panel*), and PCRA (*bottom panel*). In all panels, from *left* to *right*, we can appreciate sorLA (*green*) and cav-1 (*red*) immunostaining, the co-localized pixels channel (*white*) and the *green/red* fluorescence merged images. Co-localized pixels, highlighted in white and determined using the *Imaris x*64 6.2.0 software, reveal sorLA and cav-1 co-localization primarily at large intravesicular structures, with diffuse labeling of plasmalemma and cytoplasmic punctae. At the right hand of each panel, zoom images of large intracellular vesicular structures and plasmalemma level immunostaining are shown. Notice prominent sorLA labeling of intracellular vesicular structures consistent with its labeling of endosomes and Golgi structures. Discrete co-localization is seen at the plasmalemma level, being more evident in differentiated C6 cells. Major ticks in images are separated by 5 µm. *Scale bars* in *blue* inserts: 0.6 µm (undifferentiated C6), 1.5 µm (differentiated C6), and 0.8 µm (PCRA). *Scale bars* in *purple* inserts: 1 µm (undifferentiated C6), 1.5 µm (differentiated C6), and 1.5 µm (PCRA)

fractions obtained during density gradient centrifugation (Fig. 4), and their patterns of co-localization obtained via confocal imaging analysis (Figs. 5, 6).

Discussion

Few studies have analyzed in depth sorLA in glia. An initial study in brain tissue (Motoi et al. 1999) did not detect sorLA labeling in glia, while Scherzer et al. (2004) described no-changes in sorLA immunostaining in glia of AD patients. A third study in the literature reported downregulation of sorLA using microarrays gene analysis of human astrocytoma brains (Macdonald et al. 2007). The present study expands characterization of sorLA expression to a series of normal and transformed human and rat glia. The results presented provide evidence of its message expression in C6, PCRA, and 1321N1 astrocytoma (Fig. 1a, b). Among the latter cell lines, PCRA displays the highest levels of sorLA mRNA expression when compared to the two C6 cells (Fig. 1c). A possible explanation for the apparent discrepancy between the downregulation of sorLA expression during rat glioma differentiation and the highest levels of expression observed in primary rat astrocyte respect to tumoral cells could be associated to the differential production of neurotrophic factors between these cell types. C6 glioma cells are reactive astrocyte-like, but these are still transformed cells that can behave different to the non-tumor astrocytic phenotype observed in the embryonic PCRA. For instance, it has been shown that

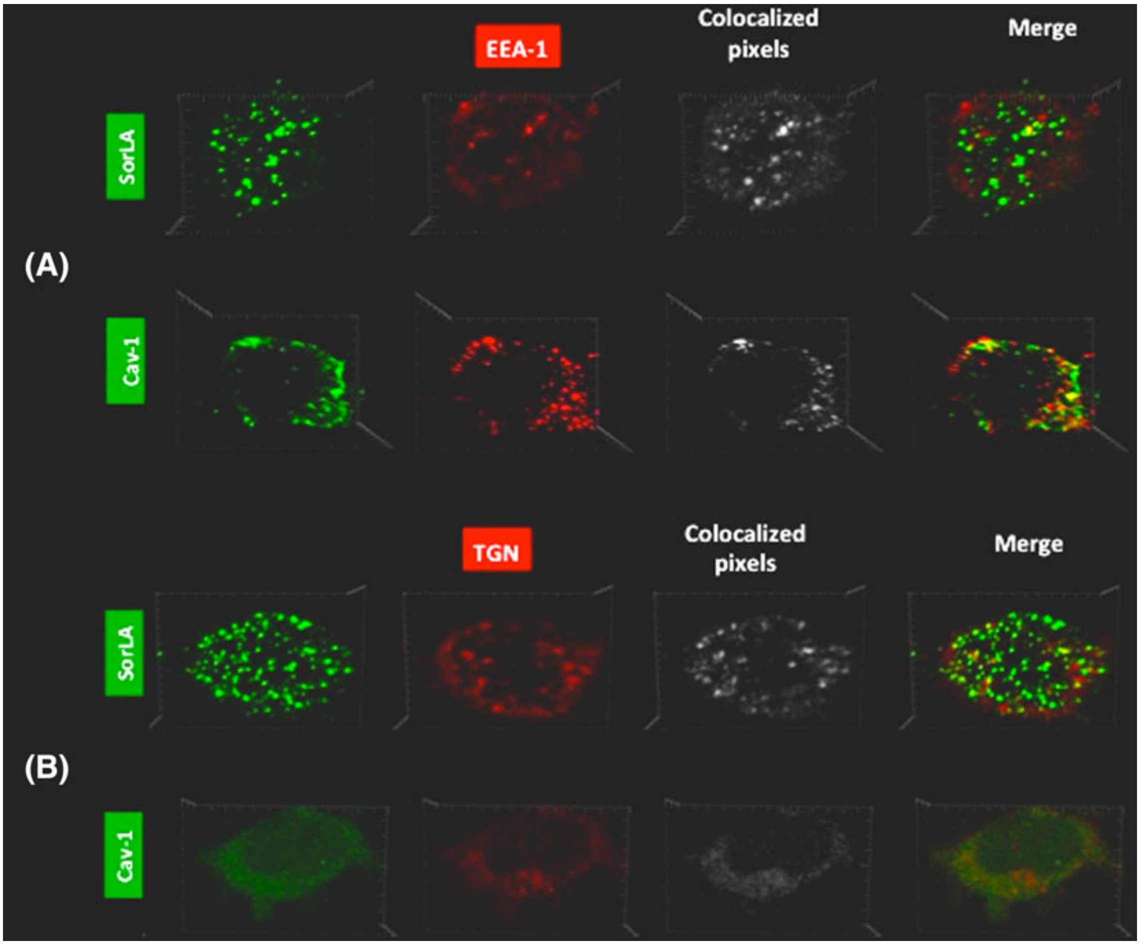

Fig. 6 Immunofluorescence co-localization analysis of sorLA and cav-1 with markers of the early endosome (EE) (EEA1) and the trans-Golgi network (TGN38) in undifferentiated C6 glioma cells. The images in **a**, from *left* to *right*, we can appreciate sorLA (*green*) and EEA-1 (*red*) immunostaining, the co-localized pixels channel (*white*) and the *green/red* fluorescence merged images. Co-localized pixels, highlighted in white and determined using the *Imaris x*64 6.2.0 software, reveal sorLA and EEA-1 co-localization in the EE compartment. Similar co-localization patterns were shown for cav-1 (*green*) and EEA-1 (*red*) immunostaining. The cav-1:EEA-1 co-localization can be appreciated in the co-localized pixels channel (*white*) and the *green/red* fluorescence merged images. Hence, both sorLA and cav-1 co-localize in the EE compartment. In the images in **b**, from *left* to *right*, we can appreciate sorLA (*green*) and TGN38 (*red*) immunostaining, the co-localized pixels channel (*white*) and the *green/red* fluorescence merged images. Co-localized pixels, highlighted in white and determined using the *Imaris* ×64 6.2.0 software, reveal sorLA and TGN38 co-localization in the TGN compartment. Similar co-localization patterns were shown for cav-1 (*green*) and TGN38 (*red*) immunostaining. The cav-1:TGN38 co-localization can be appreciated in the co-localized pixels channel (*white*) and the *green/red* fluorescence merged images. Hence, both sorLA and cav-1 can also co-localize in the TGN compartment

PCRA are associated with conditions where there is a documented elevated production of neurotrophic factor, such as the brain-derived neurotrophic factor (BDNF) (Lackland and Dreyfuss 2002). BDNF has been implicated in the upregulation of sorLA's expression (Rohe et al. 2009), since sorLA (−/−) mice treated with this neurotropic factor exhibited an increase of sorLA's transcript accompanying by a decrease of aß peptide formation.

No significant difference in transcript expression was found between the human SHSY-5Y neuroblastoma and 1321N1 astrocytoma cells. Hence, relatively higher levels of sorLA's transcript expression in PCRA, when compared to PCRN, support the need to further our characterization of its expression in this brain compartment. This scenario may be reminiscent to the enhanced expression of AD associated molecules in the glia compartment, i.e., APOE (Beffert et al. 2004; Poirier 2005) and specific APP isoforms (Gaul et al. 1992), hence underscoring the need to unravel their significance and contribution to the onset-progression of the disease.

The expression of the 250 kDa sorLA was also demonstrated by immunoblot analysis of total cell homogenates (Fig. 3) and light-density membrane raft fractions from C6 (differentiated and undifferentiated), PCRA, and 1321N1 cells (Fig. 4). In the case of C6, a significant decrease in sorLA's mRNA (Fig. 2) and protein (Fig. 3) expression is

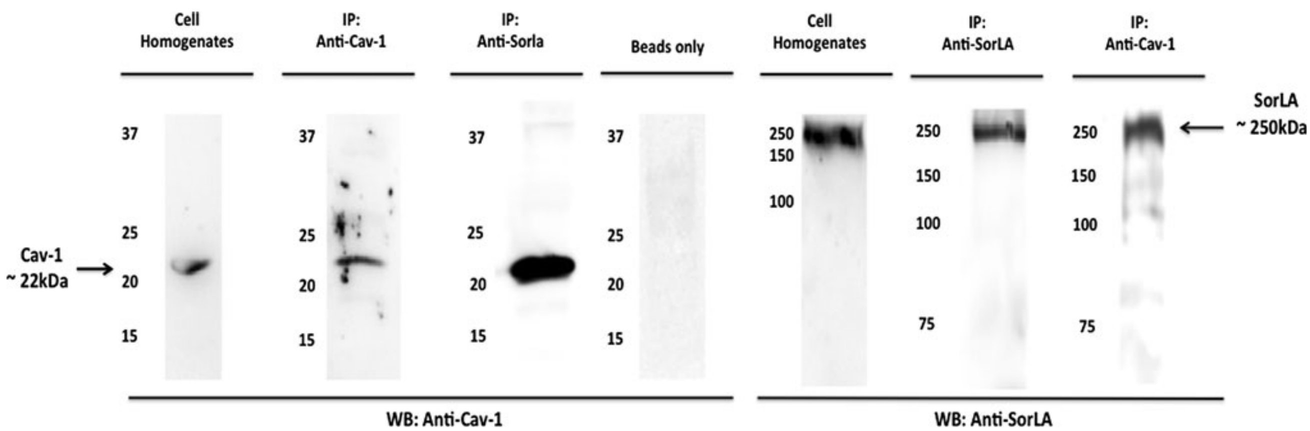

Fig. 7 Co-immunoprecipitation analysis demonstrates a direct or indirect physical interaction between sorLA and cav-1. *Left panel* displays immunoblots of membranes with an anti-cav-1 antibody, while the *right panel* represents membranes probed with an anti-sorLA antibody. The *left panel* shows in the first three strips the expected ~22 kDa band corresponding to cav-1 in total cell homogenates of undifferentiated C6 cells, and immunoprecipitates obtained using beads coupled to a cav-1 (positive control) and sorLA. The fourth strip in the *left panel* represents a negative control done with uncoupled beads only. The *right panel* shows the expected ~250 kDa band corresponding to sorLA in total cell homogenates of undifferentiated C6 cells, and immunoprecipitates obtained using beads coupled to a sorLA (positive control) and cav-1 antibody. The figure illustrates representative immunoblotblot analysis of PVDF membranes from at least four experiments in each *panel*

attained during their differentiation into an astrocyte-like phenotype. Hence, C6 differentiation permits in vitro assessment of sorLA's downregulation. Interestingly, immunoblots analysis revealed decreased sorLA expression in lymphoblast's and frontal cortex from patients with AD (Scherzer et al. 2004), and in patient subgroups with MCI (Sager et al. 2007). Although sorLA staining in glial cells seemed not to decrease, as found in the study of Scherzer et al. (2004), the relative contribution of glia in total homogenates from brain to the observed decrease cannot be determined, nor the regional variations in glial cell-specific protein expression estimated.

SorLA's downregulation, coupled to up-regulation of other factors, may generate an environment permissive of neurotoxic amyloid peptides synthesis or an increased amyloidogenic potential, both in neurons and glia. Interestingly, there is an up-regulation of cav-1 in senescent mouse and human brain (Gaudreault et al. 2004a; Kang et al. 2006); in the brain of AD patients and hippocampus of ApoE-deficient mice (Gaudreault et al. 2004a); also there is an increase in cav-1-enriched membrane raft fractions in senescent rat brain (Kang et al. 2006). Interestingly, we have previously reported cav-1 up-regulation during C6 cells differentiation (Silva et al. 2005), which coupled to the sorLA downregulation reported in this study, supports an increased cav-1:sorLA ratio attained during the differentiation process. Therefore, an increased cav-1:sorLA ratio may correlate with neurotoxic amyloid peptides synthesis. Indeed, in three distinct non-neuronal cell lines, the α-secretase-mediated proteolysis of APP was enhanced by recombinant over-expression of cav-1 and abrogated by cav-1-based antisense oligonucleotides (Ikezu et al. 1998). C6 cells, which are also known to express and process APP (Morato and Mayor 1993), may hence be used as a bioassay to study factors that can halt sorLA's "detrimental" downregulation, increase its expression, or modulate the cav-1:sorLA ratio. In this context, a most critical determinant in the neurotoxic trafficking (Huse and Doms 2001) of APP in AD may be the elevated cav-1:sorLA ratio.

Glia are thus highly relevant to our complete understanding of sorLA in AD, and permit further dissection of its trafficking by analysis of the membrane raft microdomains and association with raft-associated proteins like cav-1. This study demonstrates that sorLA displays buoyant-density properties typical of molecules associated with membrane rafts, since it co-fractionates with cav-1 and flot-2 in light-density membrane rafts fractions obtained from three different glial cell model systems (Fig. 4). This buoyant-density property of raft-associated proteins is also exhibited by APP, which co-fractionates and co-localizes with cav-1 in rat brain tissue (Kang et al. 2006), and with caveolin-3 in CRT astrocytoma membrane raft fractions (Nishiyama et al. 1999). In the case of differentiated C6 cells, it is possible that cell differentiation causes a migration of cav-1 to heavier subcellular fractions, such as high-density raft or non-raft plasmalemma microdomains, or its internalization to caveosomes (Melgren 2008). The caveosomes are higher-density cav-1-positive subcellular fractions dispersed throughout the plasma membrane and intracellular structures with irregular shapes, sizes, and a non-acidic pH (Nichols 2003). This observation is consistent and reflects the dynamic character of cav-1 positive structures.

In addition to demonstrating sorLA (mRNA and protein) expression in a series of glia and its co-fractionation with raft-associated proteins, this study demonstrates in two C6 phenotypes and PCRA (Fig. 5) that sorLA displays a subcellular distribution pattern similar to the one observed in neurons and other cell types (Motoi et al. 1999; Andersen et al. 2005; Nielsen et al. 2007). The immunostaining pattern is characterized by a diffuse dotted-punctuate labeling of cytoplasmic vesicles and the plasmalemma, with prominent labeling of larger intravesicular structures. Even more, LSCM also revealed that in both C6 phenotypes and PCRA sorLA is primarily found co-localized with cav-1 in larger intracellular vesicular compartments, and in diffusely distributed cytoplasmic vesicles (Fig. 5). Also, in all cases, discrete co-localization was seen at the plasmalemma, a region demarked in the sections shown by the presence of the CAV micropatches in C6 (Silva et al. 1999, 2005) (Fig. 5). Interestingly, plasmalemma level co-localization seemed more evident in differentiated C6 cells (Fig. 5b). This latter pattern is consistent with studies demonstrating the ability of sorLA to traffic from the trans-Golgi to plasmalemma, internalize, and be primarily found in intracellular endosomal and trans-Golgi compartments (Offe et al. 2006). Similarly, cav-1 has been found in the trans-Golgi region and in cav-1-containing endosomes (termed caveosomes) (Parton 2004; Pol et al. 1999; Pelkmans et al. 2001, 2004; Nichols 2003; Peters et al. 2003).

The present study further demonstrates that indeed, both sorLA and cav-1 co-localize with specific markers of the trans-Golgi network (TGN38) and early endosomes (EEA1) (Fig. 6). These findings strongly support the existence of a direct and/or indirect interaction between cav-1 and sorLA in their trafficking and functional fates. The indirect or direct cav-1:sorLA partnership was further demonstrated by the mutual co-immunoprecipitation of cav-1:sorLA complexes form C6 cells (Fig. 7). This interaction(s) may lead to sharing and potential modulation of their trafficking and functional roles in pathways, such as the APP amyloidogenic path.

In this context, it remains to be determined if cav-1 is part of or interacts with the retromer complex to modulate sorLA's ability to sort APP (Marcusson et al. 1994; Yamazaki et al. 1996; Jacobsen et al. 2002) away from β- and γ-secretases (Cam and Bu 2006) in late endosomal compartments (Seaman 2004; He et al. 2005) leading to decreased Aβ production (Offe et al. 2006; Spoelgen et al. 2006). Cav-1 may be a negative modulator of sorLA's function, hence leading to a scenario like retromer dysfunction, and decreased or knocked-out sorLA levels that are permissive of enhanced Aβ production (Seaman 2004; Andersen et al. 2005; He et al. 2005). Another intriguing possibility is that cav-1, and/or an increased cav-1: sorLA ratio, could facilitate progression of APP along the multivesicular body–exosomal pathway (Rajendran and Simons 2009; Rajendran et al. 2006) leading to enhanced toxic amyloid peptide biogenesis both in neurons and glia. Indeed, membrane raft markers have been found associated with the latter pathway (Rajendran et al. 2006, 2007; Schneider et al. 2008; Rajendran and Simons 2009).

Alternatively, although the intracellular co-localization of sorLA and cav-1 may be crucial in determining the amyloidogenic potential of glia, the observation of increased sorLA: cav-1 co-localization at the plasmalemma level in differentiated C6 cells (Fig. 5) suggests that interaction between sorLA and cav-1 at the plasmalemma level may lead to its "trapping" or retention and inhibition of its internalization, a necessary step for its anti-amyloidogenic action. An increased cav-1:sorLA ratio may favor this interaction and prevent sorLA from internalizing and exert its APP-retention role in the intracellular (EE and trans-Golgi) compartments, hence leading to an increased amyloidogenic potential in glia. Therefore, our findings strongly support the view that the glial compartment is an important contributor to the role of sorLA and cav-1 in AD and neurodegeneration. These findings may apply to the neuronal compartment, since cav-1 may be expressed in neurons, or raft proteins such as flotillins may exert a similar effect.

The findings presented highlight the value of the glial models systems for the study of sorLA's expression and subcellular trafficking. The dynamics unveiled could apply to neurons and non-neuronal cells. These findings also bear physiological and pathophysiological relevance leading us to acknowledge the need to consider the glial cell raft microdomains and the raft-associated protein cav-1 in our schemes on the trafficking of sorLA and its role in the processing of APP in AD. For instance, genetic variants of sorLA may need to consider cav-1 levels and mutations in AD diagnosis and treatment. It may be possible that certain cav-1 mutants or decreased cav-1 levels may offer a "neuroprotective advantage" to persons expressing sorLA mutants or decreased sorLA levels. Hence, control of glial activation could focus on the control of the cav-1:sorLA ratio as a strategy for the modulation of AD progression, or in alterations in the trafficking behavior of sorLA, since its retention (trapping) at the level of the plasmalemma or in discrete endosomal compartments by cav-1 may prevent it form exerting its anti-amyloidogenic action.

Acknowledgements This study was supported in part by the NIH-MBRS-SCORE grant S06-GM08224 awarded to WIS, and RCMI Program G12RR03051 at UPR-MSC. Graduate students IKS, JOG, and NAM were supported by the NIGMS-MBRS-RISE grant GM61838 at UPR-MSC. The authors are also grateful to Mr. Bismarck Madera for his valuable assistance with the LSCM studies.

References

Andersen OM, Reiche J, Schmidt V, Gotthardt M, Spoelgen R, Behlke J, von Arnim CA, Breiderhoff T, Jansen P, Wu X, Bales KR, Cappai R, Masters CL, Gliemann J, Mufson EJ, Hyman BT, Paul SM, Nykjaer A, Willnow TE (2005) Neuronal sorting protein-related receptor sorLA/LR11 regulates processing of the amyloid precursor protein. Proc Natl Acad Sci 102:13461–13466

Beffert U, Stolt PC, Herz J (2004) Functions of lipoprotein receptors in neurons. J Lipid Res 45:403–409

Bettens K, Brouwers N, Engelborghs S, De Deyn PP, Van Broeckhoven C, Sleegers K (2008) SORL1 is genetically associated with increased risk for late-onset Alzheimer disease in the Belgian population. Hum Mutat 29:769–770

Bujo H, Saito Y (2000) Markedly induced expression of LR11 in atherosclerosis. J Atheroscler Thromb 7:21–25

Cam JA, Bu G (2006) Modulation of beta-amyloid precursor protein trafficking and processing by the low-density lipoprotein receptor family. Mol Neurodegener 1:8

Chorna NE, Santiago-Pérez LI, Erb L, Seye C, Neary JT, Sun GY, Weisman GA, González FA (2004) P2Y2 receptors activate neuroprotective mechanisms in astrocytic cells. J Neurochem 91:119–132

Costes SV, Daelemans D, Cho EH, Dobbin Z, Pavlakis G, Lockett S (2004) Automatic and quantitative measurement of protein-protein colocalization in live cells. Biophys J 86:3993–4003

Eddleston M, Mucke L (1993) Molecular profile of reactive astrocytes: implications for their role in neurological disease. Neuroscience 54(1):15–36

Fellin T, Carmignoto G (2004) Neuron-to astrocyte signaling in the brain represents a distinct multifunctional unit. J Physiol 559: 3–15

Gaudreault S, Dea D, Poirier J (2004) Increased caveolin-1 expression in Alzheimer's disease brain. Neurobiol Aging 25(6):753–759

Gaul G, Dutly F, Frei K, Foguet M, Lübbert H (1992) APP RNA splicing is not affected by differentiation of neurons and glia in culture. FEBS Lett 307:329–332

Hansson E, Rönnbäck L (2003) Glial neuronal signaling in the central nervous system. FASEB J 17:341–348

He X, Li F, Chang WP, Tang J (2005) GGA proteins mediate the recycling pathway of memapsin 2 (BACE). J Biol Chem 280: 11696–11703

Herz J, Chen Y, Masiulis I, Zhou L (2009) Expanding functions of lipoprotein receptors. J Lipid Res 50:S287–S292

Huse J, Doms RW (2001) Neurotoxic traffic: uncovering the mechanics of amyloid production in Alzheimer's disease. Traffic 2:75–81

Ikezu T, Trapp BD, Song KS, Schlegel A, Lisanti MP, Okamoto T (1998) Caveolae, plasma membrane microdomains for α-secretase-mediated processing of the amyloid precursor protein. J Biol Chem 273:10485–10495

Jacobsen L, Madsen P, Nielsen MS, Geraerts WP, Glieman J, Smit AB, Petersen CM (2002) The sorLA cytoplasmic domain interacts with the GGA-1 and -2 and defines minimun requirements for GGA binding. FEBS Lett 511(1–3):155–158

Kanaki T, Bujo H, Hirayama S, Ishii I, Morisaki N, Schneider WJ, Saito Y (1999) Expression of LR11, a mosaic LDL receptor family member, is markedly increased in atherosclerotic lesions. Arterioscler Thromb Vasc Biol 19:2687–2695

Kang MJ, Chung YH, Hwang CI, Murata M, Fujimoto T, Mook-Jung IH, Cha CI, Park WY (2006) Caveolin-1 upregulation in senescent neurons alters amyloid precursor protein processing. Exp Mol Med 38:126–133

Kato S, Gondo T, Hoshii Y, Takahashi M, Yamada M, Ishihara T (1998) Confocal observation of senile plaques in Alzheimer's disease: senile plaque morphology and relationship between senile plaques and astrocytes. Pathol Int 48(5):332–340

Kölsch H, Jessen F, Wiltfang J, Lewczuk P, Dichgans M, Teipel SJ, Kornhuber J, Frölich L, Heuser I, Peters O, Wiese B, Kaduszkiewicz H, van den Bussche H, Hüll M, Kurz A, Rüther E, Henn FA, Maier W (2009) Association of SORL1 gene variants with Alzheimer's disease. Brain Res 1264:1–6

Lackland J., Dreyfus CF (2002) Trophins as mediators of astrocytes effects in the aging and regenerating brain. In De Vellis JS (ed) Neuroglia in the aging brain, 1st edn. Human Press, Totowa, pp 199–216

Lee JL, Cheng R, Schupf N, Manly J, Lantigua R, Stern Y, Rogaeva E, Wakutani Y, Farrer L, George-Hyslop PS, Mayeux R (2007) The association between genetic variants in sorL1 and Alzheimer's disease in an urban, multiethnic, community-based cohort. Arch Neurol 64:501–506

Livak KJ, Schmittgen TD (2001) Analysis of relative gene expression data using real-time quantitative PCR and the 2(-delta delta c(t)) method. Methods 25:402–408

Macdonald TJ, Pollack IF, Okada H, Bhattacharya S, Lyons-Weileret J (2007) Progression-associated genes in astrocytoma identified by novel microarray gene expression data reanalysis. Meth Mol Biol 377:203–221

Manders EM, Stap J, Brakenhoff GJ, van Driel R, Aten JA (1992) Dynamics of three-dimensional replication patterns during the S-phase, analyzed by double labeling of DNA and confocal microscopy. J Cell Sci 103:857–862

Marcusson E, Horazdovsky B, Cereghino J, Gharakhanian E, Emr S (1994) The sorting receptor yeast vacuolar carboxypeptidase Y is encoded by the VSP10 gene. Cell 77(4):579–586

Mattson MP, Chan SL (2003) Neuronal and glial calcium signaling in Alzheimer's disease. Cell Calcium 34:385–397

Melgren RL (2008) Detergent-resistant membrane subfractions containing proteins of plasma membrane, mitochondrial, and internal membrane origins. J Biochem Biophys Methods 70: 1029–1036

Morato E, Mayor F (1993) Production of the Alzheimer's ß-amyloid peptide by C6 glioma cells. FEBS Lett 336:275–278

Motoi Y, Aizawa T, Haga S, Nakamura S, Namba Y, Ikeda K (1999) Neuronal localization of a novel mosaic apolipoprotein E receptor, LR11, in rat and human brain. Brain Res 833: 209–215

Mrak RE, Griffin WS (2005) Glia and their cytokines in progression of neurodegeneration. Neurobiol Aging 26:349–354

Nagele RG, Wegiel J, Venkataraman V, Imaki H, Wang KC, Wegiel J (2004) Contribution of glial cells to the development of amyloid plaques in Alzheimer's disease. Neurobiol Aging 25(5):663–674

Nichols B (2003) Caveosomes and endocytosis of lipid rafts. J Cell Sci 116:4707–4714

Nielsen MS, Gustafsen C, Madsen P, Nyengaard JR, Hermey G, Bakke O, Mari M, Schu P, Pohlmann R, Dennes A, Petersen CM (2007) Sorting by the cytoplasmic domain of the amyloid precursor protein binding receptor SorLA. Mol Cell Biol 27:6842–6851

Nishiyama K, Trapp BD, Ikezu T, Ransohoff RM, Tomita T, Iwatsubo T, Kanazawa I, Hsiao KK, Lisanti MP, Okamoto T (1999) Caveolin-3 upregulation activates beta-secretase-mediated cleavage of the amyloid precursor protein in Alzheimer's disease. J Neurosci 19:6538–6548

Offe K, Dodson SE, Shoemaker JT, Fritz JJ, Gearing M, Levey AI, Lah JJ (2006) The lipoprotein receptor LR11 regulates amyloid beta production and amyloid precursor protein traffic in endosomal compartments. J Neurosci 26:1596–1603

Parton RK (2004) Caveolae meet endosomes: a stable relationship? Dev Cell 7:458–460

Pelkmans L, Kartenbeck J, Helenius A (2001) Caveolar endocytosis of simian virus 40 reveals a new two-step vesicular-transport pathway to the ER. Nat Cell Biol 3:473–483

Pelkmans L, Burli T, Zerial M, Helenius A (2004) Caveolin-stabilized membrane domains as multifunctional transport and sorting devices in endocytic membrane traffic. Cell 118:767–780

Peters PJ, Mironov A Jr, Peretz D, van Donselaar E, Leclerc E, Erpel S, DeArmond SJ, Burton DR, Williamson RA, Vey M et al (2003) Trafficking of prion proteins through a caveolae-mediated endosomal pathway. J Cell Biol 162:703–717

Pike LJ (2006) Rafts defined: a report on the keystone symposium on lipid rafts and cell function. J Lipid Res 47:1597–1598

Poirier J (1994) Apolipoprotein E in animal models of CNS injury and in Alzheimer's disease. Trends Neurosci 17:525–530

Poirier J (2005) Apolipoprotein E, cholesterol transport and synthesis in sporadic Alzheimer's disease. Neurobiol Aging 26:355–361

Pol A, Calvo M, Lu A, Enrich C (1999) The "early-sorting" endocytic compartment of rat hepatocytes is involved in the intracellular pathway of caveolin-1 (VIP-21). Hepatol 29(6): 1848–1857

Rajendran L, Simons K (2009) Membrane trafficking and targeting in Alzheimer's disease. In St George-Hyslop P et al (eds) Intracellular traffic and neurodegenerative disorders, research and perspectives in Alzheimer's Disease, Springer, Heidelberg, pp 103–113

Rajendran L, Honsho M, Zahn TR, Keller P, Geiger KD, Verkade P, Simons K (2006) Alzheimer's disease β-amyloid peptides are released in association with exosomes. Proc Natl Acad Sci 103:11172–11177

Rajendran L, Knobloch M, Geiger KD, Dienel S, Nitsch R, Simons K, Konietzko U (2007) Increased abeta production leads to intracellular accumulation of abeta in flotillin-1-positive endosomes. Neurodegener Dis 4:164–170

Reid PC, Urano Y, Kodama T, Hamakubo T (2007) Alzheimer's disease: cholesterol, membrane rafts, isoprenoids and statins. J Cell Mol Med 11:383–392

Ridet JL, Malhotra SK, Prvat A, Gage FH (1997) Reactive astrocytes: cellular and molecular cues to biological function. Trends Neurosci 20:570–577

Rogaeva E, Meng Y, Lee JH, Gu Y, Kawarai T, Zou F, Katayama T, Baldwin CT, Cheng R, Hasegawa H et al (2007) The neuronal sortilin-related receptor SORL1 is genetically associated with Alzheimer disease. Nat Genet 39:168–177

Rogaeva E, Meng Y, Lee JH, Mayeux R, Farrer LA, St George-Hyslop P (2009) The sortilin-related receptor SORL1 is functionally and genetically associated with Alzheimer's Disease. In St George-Hyslop P et al (eds) Intracellular traffic and neurodegenerative disorders, research and perspectives in Alzheimer's Disease. Springer, Berlin

Rohe M, Synowitz M, Glass R, Paul SM, Paul SM, Nykjaer A, Willnow TE (2009) Brain-derived neurotrophic factor reduces amyloidogenc processing through control of sorLA gene expression. J Neurosci 29(49):15472–15478

Sager KL, Wu J, Leurgans SE, Rees HD, Gearing M, Mufson EJ, Levey AI, Lah J (2007) Neuronal LR11/sorLA expression is reduced in mild cognitive impairment. Ann Neurol 62:640–647

Scherzer CR, Offe K, Gearing M, Rees HD, Fang G, Heilman CJ, Schaller C, Bujo H, Levey AI, Lah JJ (2004) Loss of apolipoprotein E receptor LR11 in Alzheimer disease. Arch Neurol 61:1200–1205

Schmidt V, Sporbert A, Rohe M, Reimer T, Rehm A, Andersen OM, Willnow TE (2007) SorLA/LR11 regulates processing of amyloid precursor protein via interaction with adaptors GGA and PACS-1. J Biol Chem 282:32956–32964

Schneider A, Rajendran L, Honsho M, Gralle M, Donnert G, Wouters F, Hell SW, Simons M (2008) Flotillin-dependent clustering of the amyloid precursor protein regulates its endocytosis and amyloidogenic processing in neurons. J Neurosci 28:2874–2882

Seaman MN (2004) Cargo-selective endosomal sorting for retrieval to the Golgi requires retromer. J Cell Biol 165:111–122

Selkoe DJ (2004) Cell biology of protein misfolding: the examples of Alzheimer's and Parkinson's diseases. Nat Cell Biol 6:1054–1061

Silva WI, Maldonado HM, Lisanti MP, De Vellis J, Chompre G, Mayol N, Ortiz M, Velazquez G, Maldonado A, Montalvo J (1999) Identification of caveolae and caveolin in C6 glioma cells. Int J Dev Neurosci 17:705–714

Silva WI, Maldonado HM, Velazquez G, Rubio-Davila M, Miranda JD, Aquino E, Mayol N, Cruz-Torres A, Jardón J, Salgado-Villanueva IK (2005) Caveolin isoform expression during differentiation of C6 glioma cells. Int J Dev Neurosci 23: 599–612

Silva WI, Maldonado HM, Velazquez G, Garcia JO, Gonzalez FA (2007) Caveolins in glial cell model systems: from detection to significance. J Neurochem 103S1:101–112

Sofroniew M, Vinters HV (2010) Astrocytes: biology and pathology. Acta Neuropath 119:7–35

Spoelgen R, von Arnim CA, Thomas AV, Peltan ID, Koker M, Deng A (2006) Interaction of the cytosolic domains of sorLA/LR11 with the amyloid precursor protein (APP) and beta-secretase beta-site APP-cleaving enzyme. J Neurosci 26(2):418–428

Yamazaki H, Bujo H, Kusunoki J, Seimiya K, Kanaki T, Morisaki N, Schneider WJ, Saito Y (1996) Elements of neural adhesion molecules and a yeast vacuolar protein sorting receptor are present in a novel mammalian low-density lipoprotein receptor family member. J Biol Chem 271:24761–24768